ELSEVIER

Polymer 43 (2002) 3601–3609

polymer

www.elsevier.com/locate/polymer

A polymeric solid electrolyte based on a binary blend of poly(ethylene oxide), poly(methyl vinyl ether-maleic acid) and $LiClO_4$

Ana Maria Rocco[a,*], Carla Polo da Fonseca[b], Robson Pacheco Pereira[a]

[a]*Grupo de Materiais Condutores, Instituto de Química, Universidade Federal do Rio de Janeiro, Cidade Universitaria, CT, Bloco A, 22949-900 Rio de Janeiro, RJ, Brazil*

[b]*Faculdade de Engenharia, Universidade São Fransisco, Itatiba, São Paulo, Brazil*

Received 2 October 2001; accepted 22 February 2002

Abstract

A new polymeric solid electrolyte based on a PEO/PMVE-MAc blend, complexed with $LiClO_4$, was obtained and characterized by differential scanning calorimetry (DSC), Fourier transform infrared spectroscopy (FTIR), polarized light optical microscopy, electrochemical impedance and cyclic voltammetry. DSC traces indicated miscibility for all the PSE samples. Crystallinity was suppressed for samples with $LiClO_4$ concentrations higher than 2.5 wt%. FTIR associated with DSC studies indicated that there is a preferential formation of complexes PEO/Li^+/PMVE-MAc in all PSE samples studied here. The ionic conductivity of PSE reaches a maximum of about 10^{-5} S/cm at ambient temperature and 7.5 wt% $LiClO_4$. The electrochemical stability window is 4.5 V and associated with the other characteristics, make the PSE studied here suitable for applications in 'smart-windows', batteries, sensors, etc.

Keywords: Blends; Solid electrolyte; Poly(ethylene oxide)

1. Introduction

Polymeric solid electrolytes (PSE) are complexes based on a polymer that acts as solvent for a cation. These systems show technological interest due to their application as solid electrolytes in electrochemical devices, such as energy conversion units (batteries/fuel cells) [1], electrochromic display devices and 'smart-windows' [2], photoelectrochemical cells, capacitors [3,4], etc. Among the first and most studied host for PSE is poly(ethylene oxide) (PEO), which is a polymer that dissolves high concentrations of a wide variety of salts to form polymeric electrolytes [5]. This conventional ion-conducting polymer has, in general, multiphase nature, consisting of the salt-rich crystalline phase with conductivity appreciable only above 65 °C [6], pure PEO spherulite crystalline phase, and an amorphous phase with dissolved salt. It has been revealed that the ion conduction takes place primarily in the amorphous phase and the phase diagram is affected by many factors, such as the salt species, preparation method, concentration, temperature and thermal history. At present, amorphous PEO complexes are considered to be suitable for achieving high and stable conductivity [7–9]. However, some degree of organization in the amorphous phase is required for achieving higher conductivities [10,11].

Efforts to enhance the ionic conductivity of PEO based PSE focused on suppressing its crystallization, via incorporating compounds with low T_g [12] and by copolymerization of PEO with macromonomers [13]. Copolymerization is a way to lower the melting point, modulus as well as crystallinity and to increase solubility and transparency [14]. Possible alternatives are grafting [15] and crosslinking [16], but these methods require a non-trivial synthetic process and this is a serious drawback to practical applications. It is important to develop an easier method for preparing the PSE with higher ionic conductivities and dimensional stability. In this regard, the preparation of polymeric electrolytes by blending polymers is of interest [17–20]. Blending polymers is a quick and economic alternative for obtaining materials with optimized properties and easy control of physical properties by compositional change. Work has been done on binary PEO based blends, where the second component is non-crystalline and is able to inhibit crystallization of PEO [21–23]. By blending, thermal, mechanical, and adhesive properties associated with high transparency can be optimized,

* Corresponding author. Fax: +55-21-2562-7250.
E-mail address: amrocco@iq.ufrj.br (A.M. Rocco).

0032-3861/02/$ - see front matter
PII: S0032-3861(02)00173-8

depending on the non-crystalline polymer. These properties are desired for applications in devices and they are optimized by deposition, by casting on the electrodes. This method allows one to obtain thin PSE films with good contact with the electrodes, which diminishes the time response for these devices [1].

Formation of a single phase, miscible, polymer blend usually requires the presence of favorable intermolecular interactions that contribute with a negative enthalpy to the free energy of mixing [24]. It has been reported [25,26] that PEO, because of its basic oxygen, is a good proton-accepting polymer, which allows a hydrogen bonding interaction in a blend with a proton-donor polymer.

PEO/PMVE-MAc (poly(methyl vinyl ether-maleic acid)) blends showed miscibility over the entire range of compositions studied [23]. At the molecular level it was attributed to intermolecular hydrogen bonds between the different polymers that hindered crystallization of PEO, decreasing the calculated degree of crystallinity and size of the PEO spherulites and depressing the melting point of the system. This was associated with a greater blend free volume, mobility and flexibility than in pure PEO. This system was considered a promissory host for a PSE and in this paper we report results on a solid electrolyte based on a blend of PEO, PMVE-MAc and $LiClO_4$.

2. Experimental section

2.1. Materials

The poly(methyl vinyl ether-maleic acid), PMVE-MAc ($M_w = 1.98 \times 10^6$ g/mol) and PEO ($M_w = 4 \times 10^6$ g/mol) were supplied by Aldrich Chem. Co. and have been utilized without further purification, after drying under vacuum at 50–70 °C for 48 h. Methanol (Merck, reagent grade) was distilled and stored over 4 Å molecular sieves. Anhydrous $LiClO_4$ (Aldrich) was stored under a dry atmosphere.

2.2. Sample preparation

PEO and PMVE-MAc with ratios of 60/40 wt% were dissolved in methanol with $LiClO_4$ and the solution was stirred and heated at 60 °C for 8 h. Films were prepared by casting from these solutions onto pre-heated glass plates and dried at room temperature under vacuum for 72 h. Transparent films with 1, 2.5, 5, 7.5, 10, 15 and 20 wt% $LiClO_4$ were obtained with mean thickness of ca. 200 μm as measured with a Mytotuo micrometer.

2.3. Electrochemical characterization

Stainless steel electrodes were used for electrochemical impedance measurements, which were performed in a dry box under argon (moisture content in the dry box maintained below 0.1 ppm) using a 1255 HF Schlumberger Solartron frequency response analyzer connected to a 273 PAR potentiostat. The range of analyzed frequencies was 10^{-2}–10^5 Hz. Each sample was allowed to equilibrate for 1 h at the desired temperature before measurement. The temperature range employed was 25–100 °C.

Electrochemical stability was evaluated by cyclic voltammetry in the potential range from −1 to 6.5 V vs. Li with a scan rate of 5 mV/s and at a temperature of 80 °C. The PSE films were sandwiched between a stainless steel electrode and a Li electrode. The cyclic voltammetry measurements were performed in a dry box.

2.4. Differential scanning calorimetry

To evaluate the thermal behavior of the ESP, Differential scanning calorimetry (DSC) measurements were performed on a General V4.1C DuPont 2100 apparatus. The apparatus was calibrated with an indium standard under nitrogen atmosphere. Samples were first heated from 25 to 100 °C at a heating rate of 10 °C/min (run I). In this temperature range the system is thermally stable. After a 5 min isotherm, samples were then cooled to −100 °C at the same rate (run II) and then heated at 10 °C/min to 100 °C (run III). Melting temperatures (T_m) and apparent melting enthalpy (ΔH_m) were determined from the DSC endothermic peaks on the second heating run. Glass transition temperatures (T_g) were estimated as the mean value between onset and endset temperature of the process. The melting enthalpies and temperatures were derived from the area and the maximum of the endothermic peaks, respectively. The degree of crystallinity was calculated from the following equations

$$\chi_c(\mathrm{PSE}) = \frac{\Delta H_{m,\mathrm{PSE}}}{\Delta H^0_{m,\mathrm{PSE}}} \quad (1)$$

$$\chi_c(\mathrm{PSE}) = \frac{\Delta H_{m,\mathrm{PEO}}}{\Delta H^0_{m,\mathrm{PEO}}} \quad (2)$$

where $\Delta H_{m\ \mathrm{PSE}}$, $\Delta H_{m\ \mathrm{PEO}}$ are the apparent melting enthalpies per gram of PSE and of PEO present on the PSE, respectively, and $\Delta H^0_{\mathrm{PEO}}$ is the heat of melting per gram of 100% crystalline PEO, 188 J/g [27].

2.5. Morphological studies

After 15 days, the samples deposited on glass plates were analyzed by polarized light optical microscopy (PLOM) in an Olympus BX-50.

2.6. Fourier transform infrared spectroscopy

For Fourier transform infrared spectroscopy (FTIR) spectra, samples were prepared by casting directly onto KBr pellets and films dried under vacuum. FTIR spectra were obtained on a Nicolet 760 FTIR spectrometer at room temperature. Totally 128 scans were taken with a resolution of 1 cm^{-1} and optimized gain for all samples.

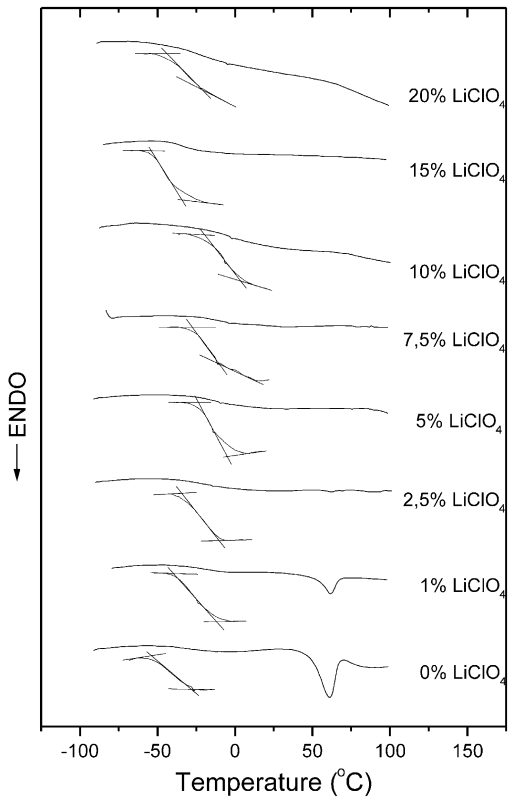

Fig. 1. DSC curves of the PSE PEO/PMVE-MAc/$LiClO_4$ for different concentrations of $LiClO_4$.

2.7. Quantitative determinations from FTIR spectra

Perchlorate anion exhibits different infrared spectra when associated in ionic pairs or dissociated, allowing one to separate different contributions from 'free' (dissociated) and 'bound' (ionic pairs or dimers) perchlorate forms [28]. The carbonyl group behaves similarly, exhibiting different bands for hydrogen bonded (or ion–dipole with Li^+) and free forms. Assuming that only these two forms (free and bound) are distinguishable in IR spectra, a deconvolution treatment was employed, using Gaussians as primitive functions. The total areas were then normalized and the ratio of free and associated forms were taken from the relative areas associated with each form.

3. Results and discussion

3.1. DSC

Fig. 1 shows the reproducible DSC curves obtained in the second heating scan for all samples, where the amplified glass transition temperature is evident. In Table 1, T_g, glass transition width (ΔT_g), melting temperature (T_m), $\Delta H_{m\ PSE}$, $\Delta H_{m\ PEO}$ and crystallinity degree, χ_c, for all the samples are shown. The films prepared as described earlier were transparent including those richer in $LiClO_4$. This property is desirable for application in smart-windows and was previously observed for the pure blends [23].

Only one T_g can be observed over the whole range of compositions studied, which indicates miscibility of the blend components in all salt composition. In comparison with the pure blend, an increase in T_g up to 10 wt% of $LiClO_4$ is observed. This suggests the formation of complexes between the polyethers and $LiClO_4$. Similar behavior was verified in recent work with PSE based on PEO–$LiClO_4$–PNNDMAA [29], and was attributed to the formation of transient crosslinks between the salt and the polyether phases, decreasing the number of hydroxyl groups participating in hydrogen bond interactions [30]. Upon further addition of the salt a decrease in T_g was observed, similar to the films of PSE of lower lithium concentration. However, for 1, 5 and 10 wt% of $LiClO_4$ an increase in ΔT_g is observed. ΔT_g is defined as the difference between the onset and endset temperatures of the glass transition process and reflects the number of relaxation processes associated with the glass transition. If the system exhibits microenvironments caused by dipole–dipole interactions or hydrogen bonding, for example, then this system should undergo relaxation processes with different relaxation times, resulting in broadening of the glass transition. In the studied PSE at least five different interactions between either of the polymer components and $LiClO_4$ can occur. These are ion–dipole interactions between lithium cations and the ether oxygen atoms in PEO and PMVE-MAc, carbonyl oxygen in PMVE-MAc, leading to the formation of complexes; hydrogen bonds of PMVE-MAc dimer [23], PMVE-MAc hydroxyl groups and ClO_4^- anions. These multiple interactions can explain the increase observed in ΔT_g. The possibility of complex formation between polyethers and alkali

Table 1
Thermal properties of the PSE PEO/PMVE-MAc/$LiClO_4$

%$LiClO_4$	T_g (°C)	ΔT_g (°C)	ΔC_p (J/°C g)	T_m (°C)	ΔH_m (J/g)	χ_c (%)
0	−29	32	0.06	63	57	30
1	−25	42	0.12	62	9	5
2.5	−22	32	0.07	62	0.5	0.3
5	−15	45	0.14	–	–	–
7.5	−13	26	0.07	–	–	–
10	−4	43	0.24	–	–	–
15	−32	29	0.11	–	–	–
20	−24	35	0.22	–	–	–

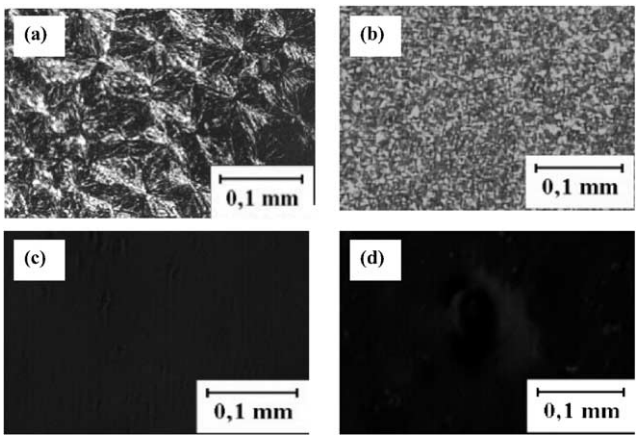

Fig. 2. PLOM of PSE samples containing (a) 0 wt% $LiClO_4$; (b) 1 wt% $LiClO_4$; (c) 2.5 wt% $LiClO_4$ and (d) 15 wt% $LiClO_4$.

metal salts is fundamental for obtaining good polymeric electrolytes.

ΔH_m decreased from 57 to 0.5 J/g from 0 to 2.5% $LiClO_4$ and for higher salt composition a melting peak cannot be detected, indicating that crystallinity was totally suppressed in these samples. It is interesting to note that the χ_c for pure blends is 30% and drastically decreases with $LiClO_4$ addition, which is another indication of a strong interaction of the salt with the polymer matrix. Nevertheless, the original miscibility of the pure blend is not affected. The T_g values retain an intermediate value between the pure polymers. This is indicative of transient crosslinking between PEO/Li^+/PMVE-MAc.

3.2. Morphological characterization

Fig. 2 shows the optical micrographs for the samples containing (a) 0, (b) 1, (c) 2.5 and (d) 15 wt% $LiClO_4$. It can be seen that for lower $LiClO_4$ concentrations, the samples present formation of small crystals, which tend to disappear for concentrations higher than 2.5 wt% of the salt. These data agree with the DSC curves obtained, in which the crystallinity is totally suppressed for $LiClO_4$ concentrations higher than 2.5 wt%.

3.3. FTIR

Introduction of a salt in a blend can change the intermolecular interactions. Among the possible interactions for the PEO/PMVE-MAc/$LiClO_4$ system, three types of relevant complexes are suggested. Type 1 complexes are those with the configuration PEO/Li^+/PEO [31], formed by Li^+ complexed with ether oxygen atoms of PEO. Type 2 complexes are those in which an interaction between a PMVE-MAc segment and a PEO segment takes place, although the presence of Li^+ could facilitate compatibilization. In this complex the original hydrogen bond interaction between PEO/PMVE-MAc in the blend could be substituted by complexation of Li^+. Type 3 complexes could be described as a PMVE-MAc/Li^+/PMVE-MAc system.

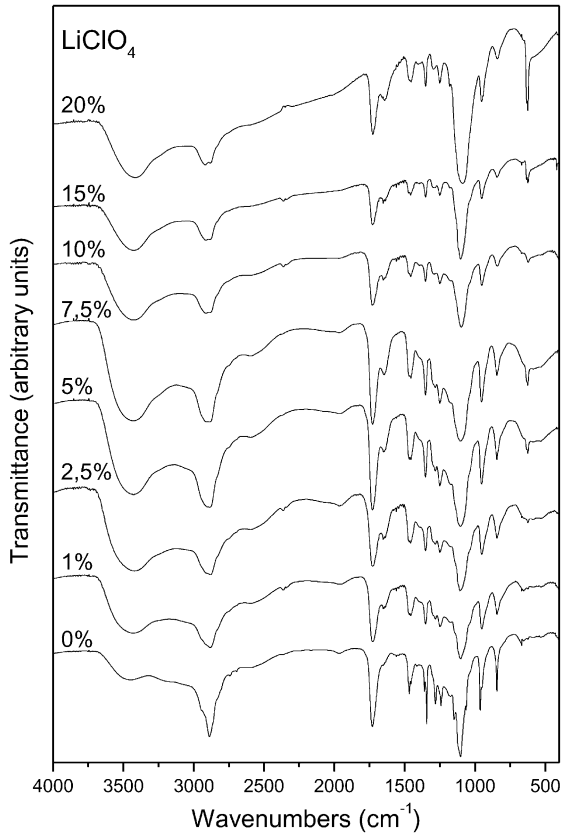

Fig. 3. FTIR spectra of the PSE for different concentrations of $LiClO_4$.

Based on the FTIR studies, we intend to elucidate the predominant micro arrangements present in the PSE. Fig. 3 shows the FTIR spectra for all samples, from 4000 to 500 cm^{-1}. Fig. 4 shows the FTIR spectra in the range of 4000–3000 cm^{-1} relative to the hydroxyl-stretching region for the 60/40 wt% PEO/PMVE-MAc blend and its PSE films with different salt concentrations. One large band centered at 3447 cm^{-1} is attributed to the stretching mode of the free and self-associated by hydrogen bonding [23] hydroxyl groups. In PSE, from 2.5 to 20 wt% $LiClO_4$, a decrease in the wavenumber from 3447 to 3421 cm^{-1} is observed, respectively. In addition to this large shift, a change in the shape of this band is evident. Changes in FTIR were attributed to interactions between the acid group of PMVE-MAc and Li^+. Since an ion–dipole interaction is stronger than a dipole–dipole interaction, a negative shift in the wavenumber takes place.

The carbonyl stretching band is shown in Fig. 5 for different concentrations of $LiClO_4$ in the PSE. For the pure blend a ν(C=O) centered at 1728 cm^{-1} corresponds to free groups and a band in the range of 1665–1600 cm^{-1} centered at 1650 cm^{-1} can be attributed to contributions of bound C=O groups in dimers of PMVE-MAc (hydrogen bound) and in ion–dipole interaction with Li^+, respectively. For the mathematical treatment, only the free and bound C=O stretching bands were considered. It was assumed that the two different contributions for the C=O bound at 1650 cm^{-1}

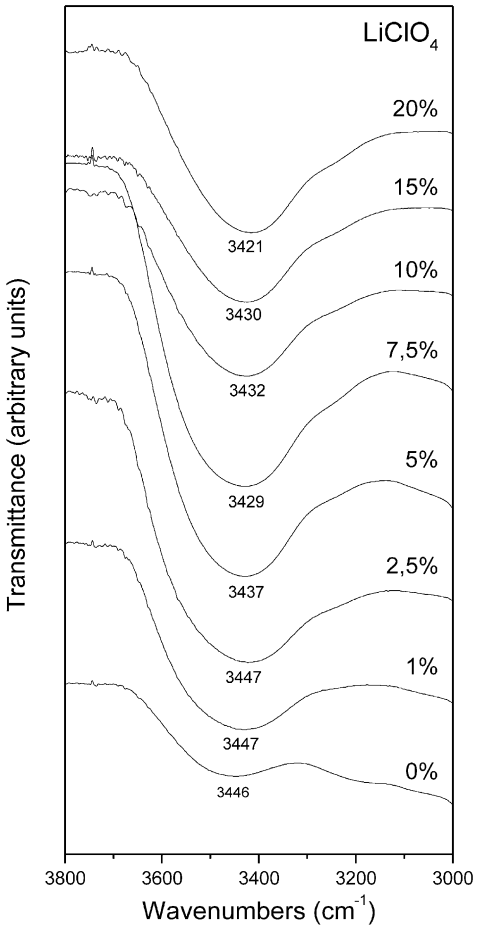

Fig. 4. FTIR spectra in the hydroxyl vibrational frequency region for the PSE samples.

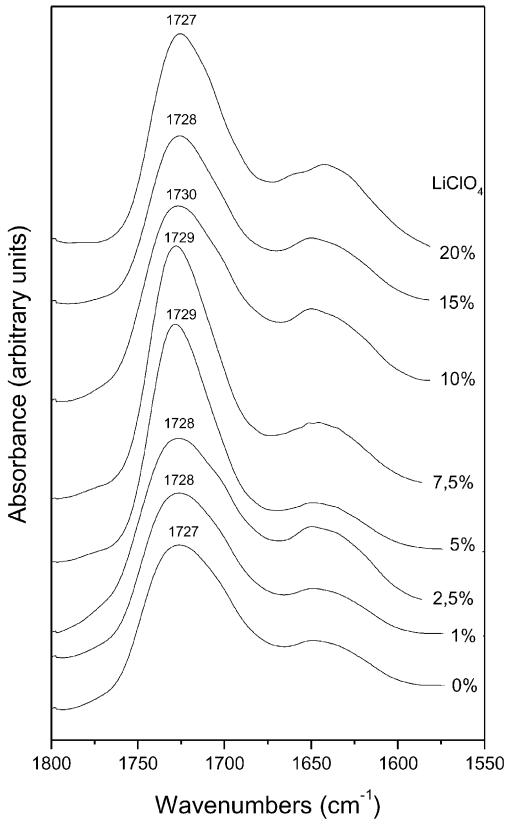

Fig. 5. FTIR spectra of the PSE in the C=O vibrational frequency region.

cannot be separated. Results of peak fitting as the ratio of spectroscopically free and associated forms is shown in Fig. 6. In this last figure it can be seen that there is a higher fraction of bound C=O groups for $LiClO_4$ concentrations below 5 wt%, whereas for higher concentrations of the salt the fraction of free and bound C=O groups is inverted, showing no variation of bound C=O groups with the $LiClO_4$ content.

The spectra in the region of the C–O–C asymmetric stretching mode for the blend of 60 wt% PEO and the PSE films are shown in Fig. 7. In the blend, a crystalline PEO phase is confirmed by the presence of the triplet peak of the C–O–C stretching vibration at 1149, 1101 and 1061 cm^{-1} with maximum at 1101. For pure PEO, this maximum is about 1109 cm^{-1} [32,33]. In the PSE spectra, changes in intensity, shape and position of the C–O–C stretching mode are associated with different micro arrangement. Apparently, the C–O–C stretching mode wavenumber remains unchanged for $LiClO_4$ concentrations up to 15 wt%. For PSE with 20 wt% $LiClO_4$, the C–O–C band maximum shifts to 1085 cm^{-1}. Probably the interactions between the basic ether oxygen of PEO and PMVE-MAc with the acid OH of PMVE-MAc in the blend are replaced by ion–dipole interaction with Li^+ in the PSE, which alters only the shape of the band for almost all salt concentrations, except for 20 wt% $LiClO_4$ where the shift of the maximum can be observed. According to Ferry et al. [34] it can be considered that there are at least two different types of sites available for the coordination of cations by PEO. In one type, cations are preferentially coordinated in a crown

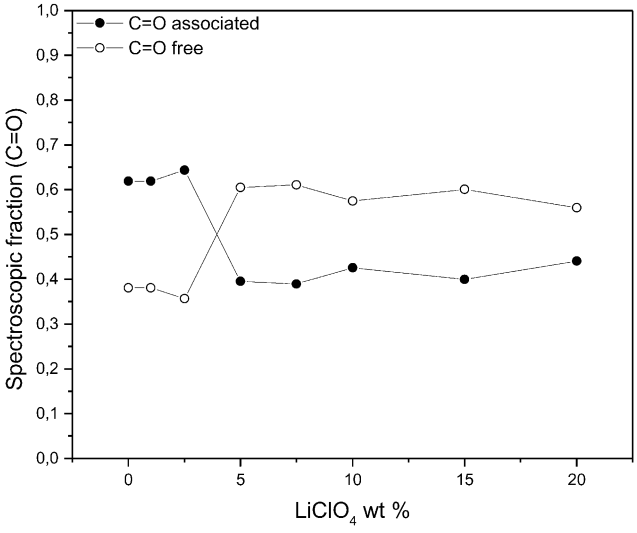

Fig. 6. Spectroscopic fraction of free (○) and bound (●) C=O as a function of $LiClO_4$ concentration.

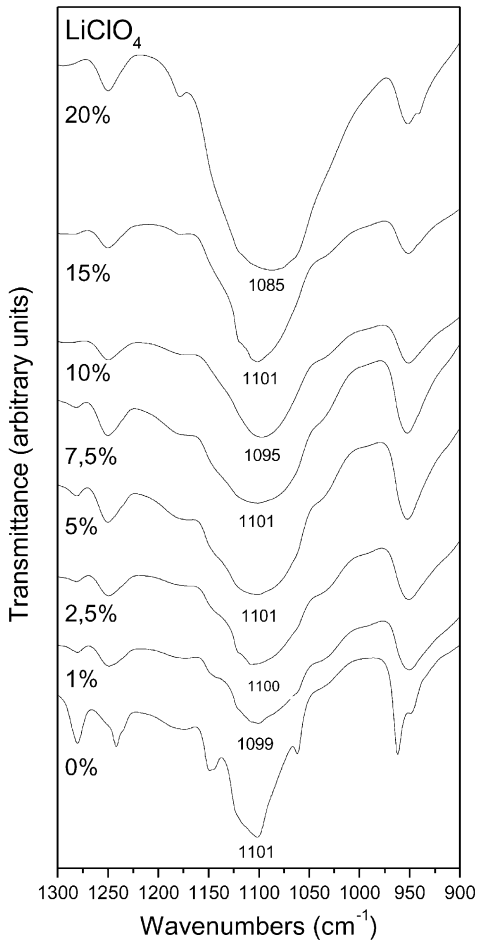

Fig. 7. FTIR spectra in the range of 1300–900 cm^{-1} (C–O–C mode).

ether configuration, and the other, cations are less tightly bound [29]. Apparently, in the PEO/PMVE-MAc/$LiClO_4$ system, the second form is predominant, probably due to the presence of a large fraction of PMVE-MAc, which may interact with PEO. The intensity of the peaks at 1144 and 1062 cm^{-1} decreases for $LiClO_4$ concentrations higher than 2.5 wt%, confirming the decrease of PEO crystallinity in the blends observed in the DSC and morphological analyses. The absence of crystallinity in all PSE samples is also shown by the disappearance of the split in the CH_2 wagging mode [29,35], observed at 1341 and 1359 cm^{-1} in the blend and at $\sim$1350 cm^{-1} in the PSE. This can be due to the interaction of PEO with Li^+ and PEO with PMVE-MAc, at all salt concentrations. Since one T_g was observed in the DSC curves, the miscibility of the blend is not affected by the presence of $LiClO_4$. Thus, Li^+ probably acts as a compatibilization agent.

Fig. 8 shows the peak fitting of the $\nu(ClO_4^-)$ mode with two separate peaks relative to the bound and free forms, with maxima at 634 and 623 cm^{-1}, respectively [29,35]. The fraction relative to the spectroscopically free and bound ClO_4^- anion, as a function of salt concentration, is shown in Fig. 9. For 1 and 2.5 wt% of $LiClO_4$, the fraction of

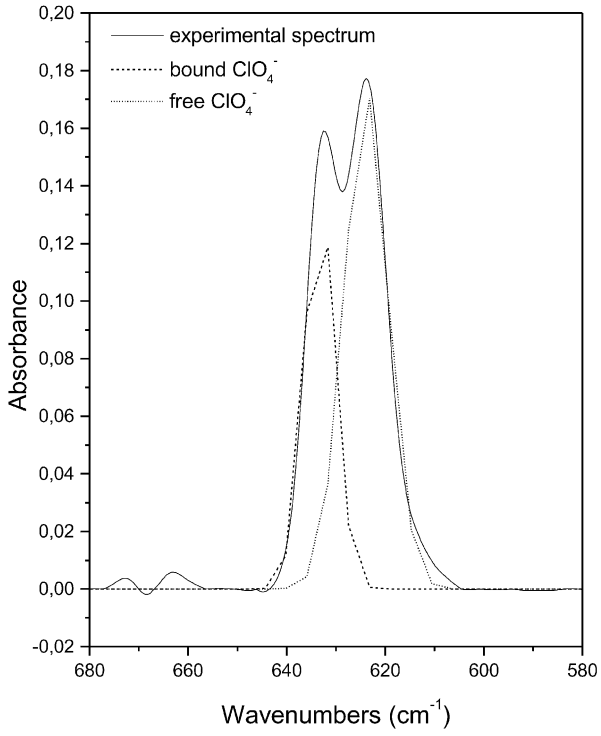

Fig. 8. Peak fitting for the ClO_4^- FTIR region for the 20 wt% $LiClO_4$ PSE.

bound ClO_4^- is higher than that of the free anion and from 5 to 10 wt% the inverse is observed with a maximum at 10 wt% $LiClO_4$. For higher concentrations, the ClO_4^- anion could be associated in $Li^+ClO_4^-$ contact ion-pairs, due to saturation of the system.

A progressive shift in the maximum of OH stretching band to lower wavenumbers with increasing $LiClO_4$ concentration is observed. This indicates that a progressively higher fraction of acid groups is involved in interactions

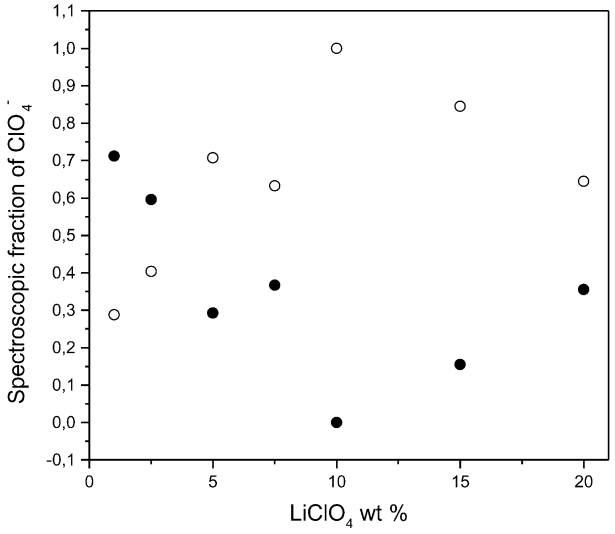

Fig. 9. Spectroscopic fraction of free (○) and bound (●) ClO_4^- as a function of $LiClO_4$ concentration.

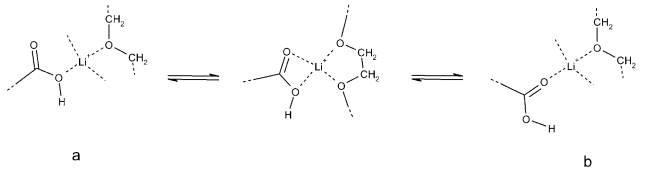

Fig. 10. Schematic structure for complexes of the type PEO/Li^+/PMVE-MAc.

of the type ion–dipole with Li^+. The OH groups forming these complexes may arise from PMVE-MAc dimers or hydrogen bonded interactions involving PMVE-MAc/PEO in the pure blend, resulting in the observed shift. On the other hand, the fraction of free C=O groups increases for $LiClO_4$ concentrations higher than 2.5 wt%, remaining unchanged up to 20 wt%. A partial replacement of PMVE-MAc dimer interactions for PMVE-MAc ion–dipole interaction with Li^+ probably takes place (Fig. 10a). This frees a fraction of the C=O groups that were hydrogen bonded in the blend, justifying its increase in the PSE. It is not possible to distinguish between the two forms of complexes (C=O···Li^+ or CO(H)···Li^+, Fig. 10b), since both of them would perturb the vibrational mode of the C=O group, and both probably occur.

Based on the FTIR and DSC studies, some conclusions can be drawn. For the Type 1 complex, a second T_g in the DSC curves, attributed to the presence of a PMVE-MAc pure phase would be expected, but it is not observed for any $LiClO_4$ concentration. Thus, there is no evidence for the preferential formation of this complex in this PSE.

For Type 2 complexes, in which an interaction between a PMVE-MAc segment and a PEO segment takes place through de Li^+, the original hydrogen bond interaction between PEO/PMVE-MAc in the blend would be substituted by complexation of both polymers with Li^+, which promotes system compatibilization. The changes observed for OH, C–O–C and C=O stretching mode support this hypothesis, and this complex could be predominant.

There is no evidence for the predominance of Type 3 complex. Similar to Type 1, a second T_g would be observed if it were present. From this we can conclude that the predominant complex formed is Type 2 (Fig. 10a and b).

3.4. EIS

In Fig. 11, the electrochemical impedance spectra of the 10 wt% $LiClO_4$ sample obtained in the temperature range from 25 to 65 °C is shown. These spectra are similar to that obtained for other PSE [36].

The different semicircle observed in the spectra is due to the conductivity of the PSE, which is strongly dependant on the temperature. The ion conduction was obtained from the intercepts of these semicircles in the abscissa. All of these spectra present a semicircle in the region of higher frequencies and an inclined line at lower ones, whose slopes do not tend to vary as a function of temperature. Under the conditions of these experiments, the semicircles represent the resistance of the electrolyte and the inclined lines indicate the resistance against ion passage in the electrolyte/electrode interface. The use of blocking electrodes for the impedance spectra results in a polarization phenomenon in the PSE bulk, since there is no ion source or sink. The electrical double layer at each interface possesses infinite resistance against ion transfer, which, in the Nyquist plot of impedance spectra, is represented by a straight line, parallel to the ordinate, associated to a limiting capacitance [32].

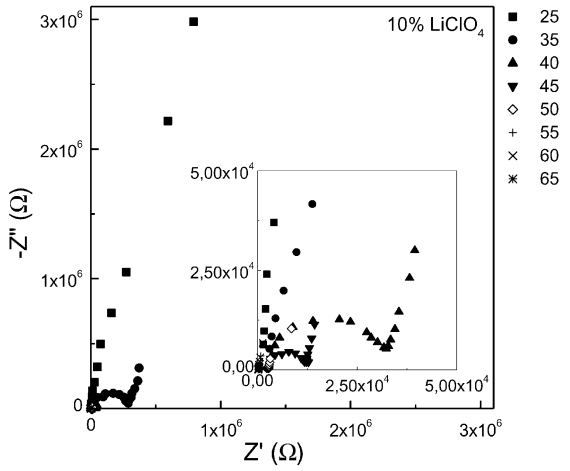

Fig. 11. Electrochemical impedance spectra of the sample 10 wt% $LiClO_4$ for temperatures from 25 to 65 °C.

Ionic conductivity (σ) values were calculated using Eq. (3) from the resistance (R) obtained at the semicircle intercept point in real axis of the impedance spectra. σ values were studied for the PSE system as a function of salt concentration and temperature. The Arrhenius model was employed for describing the temperature dependence of σ (Eq. (4)).

$$\sigma = \frac{L}{AR} \tag{3}$$

$$\log(\sigma) = \log(A) - \frac{E_a}{RT} \tag{4}$$

The dependence of conductivity, at ambient temperature, with the salt concentration is shown in Fig. 12. An increase in conductivity can be observed for $LiClO_4$ concentrations up to 10 wt%, where σ achieves approximately 10^{-5} S/cm. For samples containing 15 and 20 wt% $LiClO_4$ the conductivity decreases to approximately 10^{-7} S/cm. This behavior is coherent with the FTIR results on the deconvolution of the $\nu(ClO_4^-)$ band. The spectroscopically free form of ClO_4^-, obtained by FTIR, presents an increase with the salt concentration up to 10 wt%, similarly to the conductivity. This leads to associate: (i) the increase in conductivity with the dissociation of $LiClO_4$ into its ions in the polymeric matrix for concentrations up to 10 wt% and (ii) the decrease observed for higher (15 and 20 wt%) concentrations with

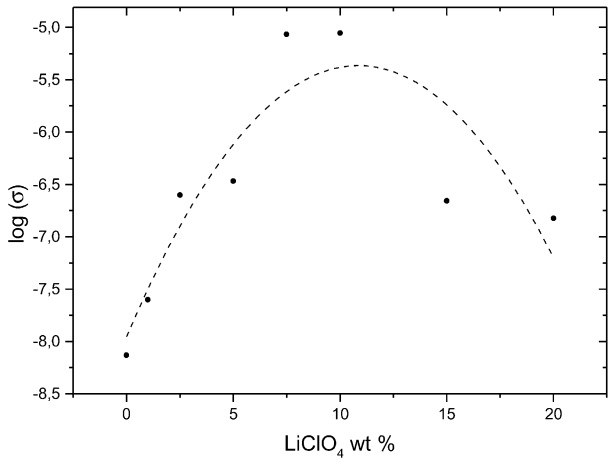

Fig. 12. Conductivity of PSE samples at room temperature as a function of the salt concentration.

the formation of ionic pairs, which decrease the number of the charge carriers. This behavior was already observed for PSE based on polyethers and alkali metal salts [37].

3.5. Arrhenius plots

The temperature dependence of conductivity is expressed in the Arrhenius plots for the samples containing 7.5 and 10 wt% $LiClO_4$ (Fig. 13). All PSE samples presented similar behavior, where conductivity increases as a function of temperature, the increase being about four orders of magnitude in the range of 15–100 °C. For higher temperatures it is expected that the polymer chains would have more mobility, with a liquid-like behavior, which would facilitate the ion transport in the PSE, raising its conductivity.

Activation energy (E_a) and log(A) values obtained from the Arrhenius plots are listed in Table 2 for the different PSE samples, where log(A) is the pre-exponential term in the Arrhenius equation and is related to the number of

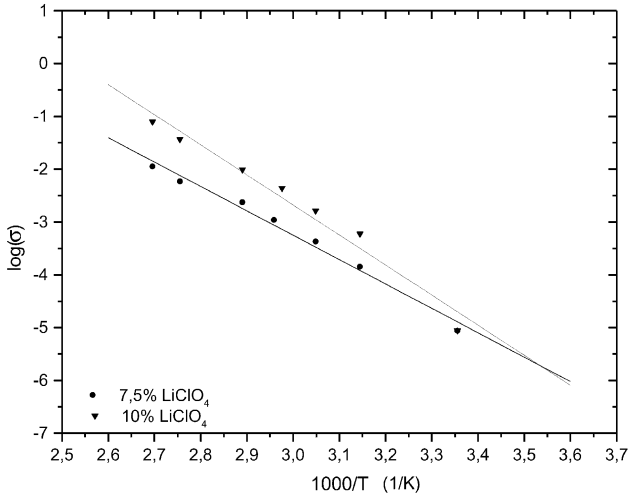

Fig. 13. Arrhenius plots of PSE samples containing 7.5 and 10 wt% $LiClO_4$.

Table 2
Activation energy (E_a), log(A) and [O]/[Li^+] ratio of the PSE PEO/PMVE-MAc/$LiClO_4$

$LiClO_4$ (wt%)	E_a (J/mol)	log(A)	[O]/[Li^+]
1	165	10.61	216
2.5	127	11.32	86
5	101	14.99	42
7.5	89	21.35	27
10	110	20.61	20
15	138	18.41	12
20	125	14.67	9

charge carriers. The values for both E_a and log(A) present a variation similar to that of the spectroscopically free ClO_4^- and of conductivity. The higher E_a was obtained for the 1 wt% $LiClO_4$ PSE, which has greater crystallinity and lower conductivity. E_a decreases for concentrations up to 7.5 wt% $LiClO_4$ (which has a higher conductivity) and than, rises again for $LiClO_4$ contents higher than 7.5 wt%. This behavior can be associated with the equilibrium between the associated and dissociated forms of $LiClO_4$. For lower salt concentrations, the number of charge carriers limits the conductivity and the crystallinity increases E_a. Increasing the salt concentration from 1 to 10 wt%, the number of charge carriers increases, since the spectroscopically free form of ClO_4^- (the dissociated ions) is predominant, increasing conductivity. The absence of crystallinity contributes to the rise of the conductivity, because it promotes greater polymer chain mobility. For $LiClO_4$ concentrations higher than 7.5 wt%, the equilibrium between the associated and dissociated forms of the salt favors the first, in accordance with the fraction of spectroscopically free and bound anions. This may promote an increase in the E_a value and a decrease in the conductivity.

As observed previously, the T_g values increases for PSE with $LiClO_4$ concentrations up to 7.5 wt%, for which the conductivity and the spectroscopically free ClO_4^- fraction reach the maximum. This increase in T_g may indicate that ion–dipole interactions are predominant and that there is a reduced tendency to form hydrogen bonds and ionically associated species. In the concentration range of 15–20 wt% $LiClO_4$, the formation of ionic pairs is favored, and the probability of formation of hydrogen bonding is increased.

3.6. Cyclic voltammetry

An important characteristic of a PSE for its technological application is the electrochemical stability window, which can be measured by cyclic voltammetry. Fig. 14 shows the cyclic voltamogram for PSE 10 wt% $LiClO_4$, which indicates that this polymeric electrolyte has an electrochemical stability window of 4.5 V vs. Li^+/Li. This potential window is wide enough for applications such as solid state capacitors and batteries.

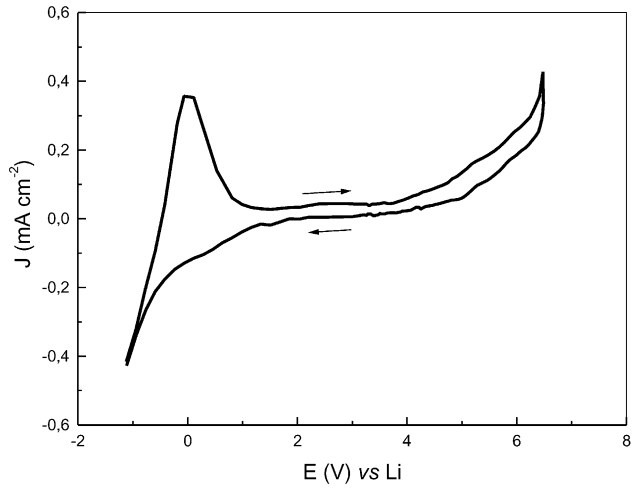

Fig. 14. Cyclic voltammogram of the system (stainless steal)/PSE/Li for the PSE with 10 wt% $LiClO_4$.

4. Conclusions

PSE based on a blend of PEO and PMVE-MAc with dissolved $LiClO_4$ have been studied over a temperature range from −100 to 100 °C using DSC, over 25–100 °C by impedance spectroscopy and at room temperature by FTIR. Salt addition suppresses the crystallinity of the blend for compositions higher than 2.5 wt% $LiClO_4$. The DSC traces showed only one T_g for all compositions in the range of temperatures studied, indicating that PMVE-MAc is distributed uniformly and inhibits PEO crystallization. Salt addition does not disturb the miscibility of the system. The ionic conductivity of the PSE reaches a maximum of approximately 10^{-5} S/cm at ambient temperature and 7.5 wt% $LiClO_4$. Upon obtaining films with thicknesses of approximately 10 μm by casting, the ohmic drop can be reduced and this conductivity (10^{-5} S/cm) suffices for many technological applications. The highest fraction of spectroscopically free ClO_4^- was observed at this concentration, indicating that the conductivity has its behavior predominantly dictated by the number of charge carriers. This fact is confirmed by the studies of the pre-exponential factor of Arrhenius, whose variation has the same tendency as that of the conductivity. FTIR associated with DSC studies indicated that there is a preferential formation of complexes between the Li^+ and the basic oxygen atoms of PEO and PMVE-MAc in all the PSE sample. This ion–dipole interaction acts as a 'crosslinking' agent between the two polymer species. It increases the T_g and promotes blend compatibilization. The electrochemical stability window is 4.5 V and along with the other characteristics, make the PSE studied suitable for applications in smart-windows, batteries, sensors, etc.

Acknowledgements

Authors would like to thank the State of Rio de Janeiro Foundation for Research Support (FAPERJ, Grant No. E-26/170414/2000) for partial support of this work and the Brazilian National Research Council (CNPq, Grant No. 522000/96-7) for fellowships (to RPP and AMR).

References

[1] Murata K, Izuchi S, Yoshihisa Y. Electrochim Acta 2000;45:1501.
[2] De Paoli M-A, Zanelli A, Mastragostino M, Rocco AM. J Electroanal Chem 1997;435:217.
[3] Mastragostino M, Arbizzani C, Meneghelo L, Paraventi R. Adv Mater 1996;4:331.
[4] Rudge A, Davey J, Raistrick I, Gottesfeld S, Ferraris JP. J Power Sources 1994;89:47.
[5] Acosta JL, Morales E. J Appl Polym Sci 1996;60:1185.
[6] Bruce PG, editor. Solid state electrochemistry. Cambridge: Cambridge University Press, 1997. p. 106.
[7] Armand MB. In: McCallum JR, Vincent CA, editors. Polymer electrolyte reviews, vol. 1. London: Elsevier Science, 1989. p. 1.
[8] Berthier C, Gorecki W, Minier M, Armand MB, Chabagno JM, Rigaud P. Solid State Ion 1983;11:91.
[9] Fauteux D, Purd'homme J, Harvey PE. Solid State Ion 1988;28:923.
[10] Dias FB, Batty SV, Gupta A, Ungar G, Voss JP, Wright PV. Electrochim Acta 1998;43:1217.
[11] Andreev YG, Bruce PG. Eletrochim Acta 2000;45:1417.
[12] Lee CC, Wright PV. Polymer 1982;23:681.
[13] Xia DW, Smid J. J Polym Sci, Polym Lett 1984;22:617.
[14] Zheng S, Huang J, Liu W, Yang X, Guo Q. Eur Polym J 1996;32:757.
[15] Su F, Feng LX, Yang SL. Appl Chem 1987;4:40.
[16] Fish D, Xia DW, Smid S. Makromol Chem 1985;6:761.
[17] Acosta JL, Morales E. Solid State Ion 1996;85:85.
[18] Kim D-W, Park JK, Rhee H-W. Solid State Ion 1996;83:49.
[19] Wieczorek W, Such K, Przyluski P, Florjanczyk Z. Synth Meth 1990; 45:373.
[20] Li J, Khen IM. Macromolecules 1993;26:4544.
[21] Herrero CR, Acosta JL. Polym J 1994;26(7):786.
[22] Cohen LE, Rocco AM. J Therm Anal Cal 2000;59:625.
[23] Rocco AM, Pereira RP, Felisberti MI. Polymer 2001;45:5199.
[24] Cowie JMG, Love C. Polymer 2001;42:4783.
[25] Coleman MKM, Moskala EJ. Polymer 1983;24:251.
[26] Berridi MJF, Valero M, Learthum AM, Espi E, Truin J. Polymer 1994;34:38.
[27] Cimmino S. Makromol Chem 1990;19:2447.
[28] Wieczoreck W, Lipka P, Zukowska G, Wycislik H. J Phys Chem B 1998;102:6968.
[29] Wieczoreck W, Raducha D, Zalewska A, Stevens JR. J Phys Chem B 1998;102:8725.
[30] Wieczoreck W, Such K, Florjanczyk Z, Stevens JR. J Phys Chem 1994;98:6840.
[31] Li J, Khan IM. Macromolecules 1993;26:4544.
[32] Li X, Hsu SL. J Polym Sci, Polym Phys Ed 1984;22:1331.
[33] Bailey Jr FE, Koleske JV. Poly(ethylene oxide). New York: Academic Press, 1976. p. 115.
[34] Ferry A, Jacobsson P, Stevens JR. J Phys Chem 1996;100:12574.
[35] Salomon M, Xu M, Eyring EM, Petrucci S. J Phys Chem 1994;98: 8234.
[36] Acosta JL, Morales E. Electrochim Acta 1998;43:791.
[37] Wu H-D, Wu I-D, Chang F-C. Polymer 2001;42:555.